

# Communication

## A 3-D Dispersive Time-Domain Meshless Formulation for Frequency-Dependent Materials

Sheyda Shams, Ali Ghafoorzadeh-Yazdi, and Masoud Movahhedi<sup>1</sup>

**Abstract**—This communication presents a novel transient meshless formulation for analyzing wave propagation through linear dispersive materials. Many real materials are linear dispersive; thus, their constitutive parameters are not constant and change with frequency. However, the conventional numerical techniques are not proper tools for numerical analysis of dispersive materials, considering that they are formulated based on the assuming constant constitutive parameters for the materials. Therefore, until now, a number of numerical techniques have been proposed for modeling frequency behavior of dispersive materials. On the other hand, meshless methods are new and powerful numerical techniques which their capability in simulating the problem domain without using connection information among nodes makes them efficient techniques for modeling problems with complex geometries. In this communication, we have demonstrated that by incorporating some approaches into the meshless methods, we can turn them into suitable tools for modeling dispersive media. In order to obtain a meshless analysis of a dispersive medium, we have considered the scalar radial basis function meshless method, and for taking the frequency behavior of the medium into account, the auxiliary differential equations method has been used. Hence, the proposed dispersive meshless method not only models the frequency behavior of the dispersive materials but also provides more flexibility in simulating problems with complex geometries. In addition, the efficiency and accuracy of our proposed method are investigated by two numerical examples.

**Index Terms**—Auxiliary differential equations (ADEs) method, dispersive materials, dispersive meshless method, meshless method.

### I. INTRODUCTION

The time-domain numerical techniques have attracted a great attention among other numerical methods, particularly because of their ability in simulating problems over a wide frequency band. The dielectric properties (permittivity, permeability, and conductivity) of many real materials vary significantly with frequency [1]. However, usually these variations are not included in conventional time-domain numerical methods due to consideration of the constitutive parameters as constants. Hence, the time-domain analysis of dispersive materials with suitable numerical methods is of considerable importance. For a frequency-dependent or linear dispersive medium which its constitutive parameters are not constant over a wide frequency spectrum, the nondispersive calculation leads to precise results only at or near the center of the frequency band of interest, but the accuracy will be decreased at other frequencies [2]. Therefore, to obtain more accurate results in simulating dispersive media over a wide frequency spectrum, it is often required to model the dielectric properties of the materials by a more precise dispersion model which includes the frequency behavior of the medium.

In order to analyze wave propagation through linear dispersive media, several approaches have been incorporated into some time-

domain numerical techniques such as the finite-difference time-domain (FDTD) method [3] and finite-element method (FEM) [4]. These approaches are classified into three categories in most of the references. Three general types of algorithms which have merged into FDTD method are known as *recursive convolution (RC)*, *auxiliary differential equation (ADE)*, and *Z-transform* approaches. Using the *RC* approach, in 1990, Luebbers *et al.* [5] published the first frequency-dependent FDTD formulation. In addition, Bui *et al.* [6], Hawkins and Kallman [7], Hunsberger *et al.* [8], Pontalti *et al.* [9], and Melon *et al.* [10] used the *RC* FDTD approach to model different dispersive media. In the *RC* approach, the susceptibility function can be described for many materials by an exponential function and the electric-flux or magnetic-flux densities are related to the electric field intensity or magnetic field intensity, respectively, through a convolution integral.

In the *ADE* method, the electric-flux density is related to the electric field intensity by an *ADE*. Kashiwa *et al.* [11], Kashiwa and Fukai [12], Joseph *et al.* [13], and Gandhi *et al.* [14] are some researchers who utilized the *ADE* approach to model dispersive media. In 1992, Sullivan [15] applied the *Z-transform* to Maxwell's equations and proposed the *Z-transform* approach for modeling dispersive media.

Conventional grid-based numerical methods, such as the FDTD method, are efficient tools for transient electromagnetic analysis. However, these methods despite of their strengths suffer from some limitations. As an example for FDTD and FEM numerical analysis of problems with complex geometries, discretization scheme is encountered with some difficulties. The time-domain meshless method [16] is a new powerful numerical method for analyzing electromagnetic problems over a broad spectrum. This method due to its capability in representation of the problem domain, and its boundary without using a mesh has recently gained much attention among other time-domain numerical techniques.

In spite of capabilities of meshless methods specially in modeling problems with complex geometries, until now, the authors have seen no reports about applying any approaches to the meshless method for analyzing dispersive media. Therefore, in this communication, we have illustrated that by incorporating some approaches into the meshless method, it can be transformed into an efficient tool for analyzing electromagnetic propagation through linear dispersive materials. In this communication, we have approximated spatial derivatives in Maxwell's equations by the radial basis function (RBF) meshless method [17], and an explicit finite-difference scheme is used to discretize time derivatives. Kansa [18] have proposed RBF method as a powerful tool to solve partial differential equations. We have considered the RBF meshless method among other meshless methods because it is an efficient technique to solve time-domain electromagnetic problems. Moreover, we have applied *ADE* technique to incorporate frequency dispersion into the scalar RBF meshless method. The linear dispersive materials can be categorized into three important generic types: Debye, Lorentz, and Drude materials [3]. In this communication, we have applied the proposed dispersive

Manuscript received November 22, 2016; revised June 10, 2017; accepted December 4, 2017. Date of publication December 18, 2017; date of current version February 1, 2018. (Corresponding author: Masoud Movahhedi.)

The authors are with the Department of Electrical Engineering, Yazd University, Yazd 89195-741, Iran (e-mail: sh.shams70@gmail.com; sh.shams@stu.yazd.ac.ir; aghafoorzadeh@yazd.ac.ir; movahhedi@yazd.ac.ir).

Color versions of one or more of the figures in this communication are available online at <http://ieeexplore.ieee.org>.

Digital Object Identifier 10.1109/TAP.2017.2784443

0018-926X © 2017 IEEE. Personal use is permitted, but republication/redistribution requires IEEE permission.

See [http://www.ieee.org/publications\\_standards/publications/rights/index.html](http://www.ieee.org/publications_standards/publications/rights/index.html) for more information.

meshless method for the study of wave propagation through media with Drude dispersion model.

The ADEs method is a simple and efficient technique for modeling a frequency-dependent medium [19]. Until now, different algorithms involving ADEs have been proposed for applying to the conventional FDTD method. Gandhi *et al.* [20] have proposed a different ADE approach, namely,  $(\mathbf{E}, \mathbf{D}, \mathbf{H}, \mathbf{B})$  scheme which links the electromagnetic flux densities and the electromagnetic field intensities for the analysis of general dispersive medium. Hao and Mittra [19] have applied the  $(\mathbf{E}, \mathbf{D}, \mathbf{H}, \mathbf{B})$  scheme which is based on the proposed ADE method in [20] for FDTD modeling of the media with Drude dispersion model. In order to derive our formulation, we have incorporated the ADE formulation of [19] into the meshless method.

In the following sections, we will first give a brief description of scalar RBF meshless method. Then, the details of the formulation of our proposed dispersive meshless method will be explained. In Section IV two numerical examples are presented to verify the efficiency and accuracy of the proposed method. Finally, conclusions are drawn in Section V.

## II. MESHLESS SCALAR RBF METHOD

The RBF method which was proposed by Kansa [18] has been extended to analyze transient electromagnetic problems in [17]. In order to interpolate an unknown function (i.e.,  $u$  in our case) in a problem, the spatial domain and its boundary should be first represented by a set of nodes scattered in the problem domain. Then, the function value of the mentioned unknown function  $u$  at a point of interest in the spatial domain can be interpolated by the RBF as follows [4]:

$$u(\mathbf{x}) = \sum_{j=1}^N \phi(\|\mathbf{x} - \mathbf{x}_j\|) a_j \quad (1)$$

where  $\mathbf{x} = (x, y, z)$  is the location of the point of interest,  $\mathbf{x}_j = (x_j, y_j, z_j)$  is the location of the node  $j$ ,  $N$  is the number of nodes within the support domain of the point of interest at which  $u$  is to be interpolated,  $a_j$  are the unknown expansion coefficients, and  $\phi(\|\mathbf{x} - \mathbf{x}_j\|)$  is the RBF. Four typical types of RBFs are the multiquadrics function, the Gaussian (Exp) function, the thin plate spline function, and the Logarithmic RBF [16]. We consider the Gaussian function as the RBF, which is formulated as follows [4]:

$$\phi_j = \phi(\|\mathbf{x} - \mathbf{x}_j\|) = e^{-\alpha r^2} \quad (2)$$

where  $r = \sqrt{(x - x_j)^2 + (y - y_j)^2 + (z - z_j)^2}$  is the variable of the RBF and  $\alpha$  is the shape parameter of the Gaussian function. Any RBFs have one or several shape parameters which adjust the performance of the functions. The unknown expansion coefficients can be determined by enforcing (1) to be satisfied at each scattered node in the support domain of the point of interest at  $\mathbf{x}$ . This leads to one linear equation for each node and finally  $n$  linear equations will obtain [16]. The compact matrix form of the obtained equations is as follows:

$$\mathbf{A} \cdot \mathbf{a} = \mathbf{u}_s \quad (3)$$

where  $\mathbf{u}_s = [u_1 \ u_2 \ \dots \ u_N]^T$  is the vector which contains the value of function  $u$  at node  $j$  ( $j = 1, 2, \dots, N$ ),  $\mathbf{a} = [a_1 \ a_2 \ \dots \ a_N]^T$  is the unknown vector of coefficients for RBF, and

$$\mathbf{A} = \begin{bmatrix} \phi(\|\mathbf{x}_1 - \mathbf{x}_1\|) & \phi(\|\mathbf{x}_1 - \mathbf{x}_2\|) & \dots & \phi(\|\mathbf{x}_1 - \mathbf{x}_N\|) \\ \phi(\|\mathbf{x}_2 - \mathbf{x}_1\|) & \phi(\|\mathbf{x}_2 - \mathbf{x}_2\|) & \dots & \phi(\|\mathbf{x}_2 - \mathbf{x}_N\|) \\ \vdots & \vdots & \ddots & \vdots \\ \phi(\|\mathbf{x}_N - \mathbf{x}_1\|) & \phi(\|\mathbf{x}_N - \mathbf{x}_2\|) & \dots & \phi(\|\mathbf{x}_N - \mathbf{x}_N\|) \end{bmatrix} \quad (4)$$

By solving (3), the expansion coefficients  $a_j$  can be calculated. Substitution of  $a_j$  into (1) leads to approximate the unknown field variable  $u$  by the vector of shape functions  $\Phi$  as

$$u = \mathbf{B}\mathbf{A}^{-1}\mathbf{u}_s = \Phi\mathbf{u}_s \quad (5)$$

where  $\Phi = [\Phi_1 \ \Phi_2 \ \dots \ \Phi_N] = \mathbf{B}\mathbf{A}^{-1}$  is the vector of shape function and contains  $\Phi_j = \Phi_j(\|\mathbf{x} - \mathbf{x}_j\|)$  as the shape function of spatial node  $j$  ( $j = 1, 2, \dots, N$ ),  $\mathbf{u}_s$  is the vector which contains the known field variable associated with spatial node  $j$ , and  $\mathbf{B} = \mathbf{B}(\|\mathbf{x} - \mathbf{x}_j\|) = [\phi_1 \ \phi_2 \ \dots \ \phi_N]$  is the vector which contains the RBFs.

The partial derivatives of shape function can be analytically calculated. The first-order partial derivatives can be obtained as

$$\frac{\partial \Phi}{\partial \kappa} = \frac{\partial \mathbf{B}(\|\mathbf{x} - \mathbf{x}_j\|)}{\partial \kappa} \mathbf{A}^{-1} \quad (6)$$

where  $\partial \kappa$  denotes a partial differentiation with respect to the spatial coordinates  $x$ ,  $y$ , or  $z$ .

By obtaining the partial derivatives of shape function, partial derivatives of  $u(\mathbf{x})$  can be found as

$$\frac{\partial u(\mathbf{x})}{\partial \kappa} = \frac{\partial \Phi}{\partial \kappa} \mathbf{u}_s. \quad (7)$$

## III. FORMULATION OF THE PROPOSED 3-D DISPERSIVE TIME-DOMAIN MESHLESS METHOD WITH AUXILIARY DIFFERENTIAL EQUATIONS

In order to obtain the meshless analysis of each electromagnetic problem, the problem domain must be represented with a set of electric field nodes and a set of magnetic field nodes. These nodes must be arranged in such a way that each electric field node be surrounded by magnetic field nodes and vice versa [21]. Moreover, in the meshless method despite of the FDTD method which is based on Yee's algorithm, all components of the electric fields are located at the same electric field nodes and the magnetic field components are located at the same magnetic field nodes.

For analyzing a dispersive material through our proposed dispersive meshless method, there is a difference in the process of space domain representation of the medium. In this method, we utilize the electric-flux density vector  $\mathbf{D}$  and magnetic-flux density vector  $\mathbf{B}$  for obtaining auxiliary equations and modeling the frequency behavior of the medium. Therefore, in order to represent the space domain, a set of electric-flux density nodes and a set of magnetic-flux density nodes in addition to the electric and magnetic field nodes must be considered. In addition, all components of the electric-flux density vector are located at the same electric field nodes and the magnetic-flux density vector components are placed at the same magnetic field nodes.

In a problem domain that has no electric or magnetic current sources, the scalar Maxwell's equations in differential form are specified by

$$\frac{\partial D_x}{\partial t} = \frac{\partial H_z}{\partial y} - \frac{\partial H_y}{\partial z} \quad (8)$$

$$\frac{\partial D_y}{\partial t} = \frac{\partial H_x}{\partial z} - \frac{\partial H_z}{\partial x} \quad (9)$$

$$\frac{\partial D_z}{\partial t} = \frac{\partial H_y}{\partial x} - \frac{\partial H_x}{\partial y} \quad (10)$$

$$\frac{\partial B_x}{\partial t} = \frac{\partial E_y}{\partial z} - \frac{\partial E_z}{\partial y} \quad (11)$$

$$\frac{\partial B_y}{\partial t} = \frac{\partial E_z}{\partial x} - \frac{\partial E_x}{\partial z} \quad (12)$$

$$\frac{\partial B_z}{\partial t} = \frac{\partial E_x}{\partial y} - \frac{\partial E_y}{\partial x} \quad (13)$$

In analysis of dispersive materials, the frequency behavior of the medium is modeled by a dispersion model to provide a more accurate approximation to the complex constant permittivity and permeability. We consider Drude linear dispersion model for both the permittivity and permeability with identical dispersion forms. Extension to the other dispersion models will remain as an open problem for our future research.

In the ADEs scheme, by considering Drude dispersion model for the permittivity and permeability of the dispersive medium, the electric-flux and magnetic-flux densities are related to the electric field and magnetic field, respectively, as follows [19]:

$$D_x = \varepsilon_0 \left( 1 - \frac{\omega_{ep}^2}{\omega^2 - j\gamma_e\omega} \right) E_x \quad (14)$$

$$D_y = \varepsilon_0 \left( 1 - \frac{\omega_{ep}^2}{\omega^2 - j\gamma_e\omega} \right) E_y \quad (15)$$

$$D_z = \varepsilon_0 \left( 1 - \frac{\omega_{ep}^2}{\omega^2 - j\gamma_e\omega} \right) E_z \quad (16)$$

$$B_x = \mu_0 \left( 1 - \frac{\omega_{mp}^2}{\omega^2 - j\gamma_m\omega} \right) H_x \quad (17)$$

$$B_y = \mu_0 \left( 1 - \frac{\omega_{mp}^2}{\omega^2 - j\gamma_m\omega} \right) H_y \quad (18)$$

$$B_z = \mu_0 \left( 1 - \frac{\omega_{mp}^2}{\omega^2 - j\gamma_m\omega} \right) H_z \quad (19)$$

where  $\omega_{ep}$  and  $\omega_{mp}$  are the electric and magnetic plasma frequencies, respectively, also  $\gamma_e$  and  $\gamma_m$  are the corresponding collision frequencies.

In order to obtain (14)–(19) in the time domain, we have to calculate the inverse Fourier transform of these equations. Since in the frequency-domain multiplication of  $j\omega$  is equivalent to the time derivatives in the time domain, the mentioned equations in the time domain are as follows:

$$\frac{\partial^2 D_x}{\partial t^2} + \gamma_e \frac{\partial D_x}{\partial t} = \varepsilon_0 \frac{\partial^2 E_x}{\partial t^2} + \varepsilon_0 \gamma_e \frac{\partial E_x}{\partial t} + \varepsilon_0 \omega_{ep}^2 E_x \quad (20)$$

$$\frac{\partial^2 D_y}{\partial t^2} + \gamma_e \frac{\partial D_y}{\partial t} = \varepsilon_0 \frac{\partial^2 E_y}{\partial t^2} + \varepsilon_0 \gamma_e \frac{\partial E_y}{\partial t} + \varepsilon_0 \omega_{ep}^2 E_y \quad (21)$$

$$\frac{\partial^2 D_z}{\partial t^2} + \gamma_e \frac{\partial D_z}{\partial t} = \varepsilon_0 \frac{\partial^2 E_z}{\partial t^2} + \varepsilon_0 \gamma_e \frac{\partial E_z}{\partial t} + \varepsilon_0 \omega_{ep}^2 E_z \quad (22)$$

$$\frac{\partial^2 B_x}{\partial t^2} + \gamma_m \frac{\partial B_x}{\partial t} = \mu_0 \frac{\partial^2 H_x}{\partial t^2} + \mu_0 \gamma_m \frac{\partial H_x}{\partial t} + \mu_0 \omega_{mp}^2 H_x \quad (23)$$

$$\frac{\partial^2 B_y}{\partial t^2} + \gamma_m \frac{\partial B_y}{\partial t} = \mu_0 \frac{\partial^2 H_y}{\partial t^2} + \mu_0 \gamma_m \frac{\partial H_y}{\partial t} + \mu_0 \omega_{mp}^2 H_y \quad (24)$$

$$\frac{\partial^2 B_z}{\partial t^2} + \gamma_m \frac{\partial B_z}{\partial t} = \mu_0 \frac{\partial^2 H_z}{\partial t^2} + \mu_0 \gamma_m \frac{\partial H_z}{\partial t} + \mu_0 \omega_{mp}^2 H_z. \quad (25)$$

Now with the defined nodes, in order to discretization of (8)–(13) in the time and space, we approximate the time derivatives in Maxwell's equations by central finite-difference scheme and apply RBF meshless method for interpolating the space derivatives. The following equations are obtained:

$$D_{x,i}^{n+1} = D_{x,i}^n + \Delta t \left( \sum_j H_{z,j}^{n+1/2} \partial_y \Phi_j - \sum_j H_{y,j}^{n+1/2} \partial_z \Phi_j \right) \quad (26)$$

$$D_{y,i}^{n+1} = D_{y,i}^n + \Delta t \left( \sum_j H_{x,j}^{n+1/2} \partial_z \Phi_j - \sum_j H_{z,j}^{n+1/2} \partial_x \Phi_j \right) \quad (27)$$

$$D_{z,i}^{n+1} = D_{z,i}^n + \Delta t \left( \sum_j H_{y,j}^{n+1/2} \partial_x \Phi_j - \sum_j H_{x,j}^{n+1/2} \partial_y \Phi_j \right) \quad (28)$$

$$B_{x,i}^{n+3/2} = B_{x,i}^{n+1/2} + \Delta t \left( \sum_j E_{y,j}^{n+1} \partial_z \Phi_j - \sum_j E_{z,j}^{n+1} \partial_y \Phi_j \right) \quad (29)$$

$$B_{y,i}^{n+3/2} = B_{y,i}^{n+1/2} + \Delta t \left( \sum_j E_{z,j}^{n+1} \partial_x \Phi_j - \sum_j E_{x,j}^{n+1} \partial_z \Phi_j \right) \quad (30)$$

$$B_{z,i}^{n+3/2} = B_{z,i}^{n+1/2} + \Delta t \left( \sum_j E_{x,j}^{n+1} \partial_y \Phi_j - \sum_j E_{y,j}^{n+1} \partial_x \Phi_j \right) \quad (31)$$

where  $\partial_x \Phi_j$ ,  $\partial_y \Phi_j$ , and  $\partial_z \Phi_j$  denote the partial differentiation of the shape function of meshless method with respect to the spatial coordinates  $x$ ,  $y$ , and  $z$ , respectively.

In order to discretize the first and second-order time derivatives of the electric field, the magnetic field, the electric-flux density, and the magnetic-flux density in (20)–(25), we apply a second-order accurate central-difference scheme centered at time-step  $n$  as [19]

$$\frac{\partial F}{\partial t} = \frac{F^{n+1} - F^{n-1}}{2\Delta t} \quad (32)$$

$$\frac{\partial^2 F}{\partial t^2} = \frac{F^{n+1} - 2F^n + F^{n-1}}{(\Delta t)^2}. \quad (33)$$

Here, we have used  $F$  to represent each component of the mentioned quantities. Then, we approximate the remaining fields ( $E_x$ ,  $E_y$ ,  $E_z$ ,  $H_x$ ,  $H_y$ , and  $H_z$ ) by a semi-implicit scheme as [19]

$$F = \frac{F^{n+1} + 2F^n + F^{n-1}}{4}. \quad (34)$$

By applying (32)–(34) to (20)–(25), the discretized equations in the time domain are obtained as

$$E_{x,i}^{n+1} = \sum_{m=0}^M b_m D_{x,i}^{n-m+1} - \sum_{m=1}^M a_m E_{x,i}^{n-m+1} \quad (35)$$

$$E_{y,i}^{n+1} = \sum_{m=0}^M b_m D_{y,i}^{n-m+1} - \sum_{m=1}^M a_m E_{y,i}^{n-m+1} \quad (36)$$

$$E_{z,i}^{n+1} = \sum_{m=0}^M b_m D_{z,i}^{n-m+1} - \sum_{m=1}^M a_m E_{z,i}^{n-m+1} \quad (37)$$

$$H_{x,i}^{n+3/2} = \sum_{m=0}^M d_m B_{x,i}^{n-m+3/2} - \sum_{m=1}^M c_m H_{x,i}^{n-m+3/2} \quad (38)$$

$$H_{y,i}^{n+3/2} = \sum_{m=0}^M d_m B_{y,i}^{n-m+3/2} - \sum_{m=1}^M c_m H_{y,i}^{n-m+3/2} \quad (39)$$

$$H_{z,i}^{n+3/2} = \sum_{m=0}^M d_m B_{z,i}^{n-m+3/2} - \sum_{m=1}^M c_m H_{z,i}^{n-m+3/2} \quad (40)$$

where  $M = 2$  and coefficients are expressed as

$$a_1 = \frac{2\varepsilon_0 \Delta t^2 \omega_{ep}^2 - 8\varepsilon_0}{A} \quad (41)$$

$$a_2 = \frac{4\varepsilon_0 - 2\Delta t \varepsilon_0 \gamma_e + \varepsilon_0 \Delta t^2 \omega_{ep}^2}{A} \quad (42)$$

$$b_1 = \frac{-8}{A} \quad (43)$$

$$b_0 = \frac{4 + 2\Delta t \gamma_e}{A} \quad (44)$$

$$b_2 = \frac{4 - 2\Delta t \gamma_e}{A} \quad (45)$$

$$A = 4\epsilon_0 + 2\Delta t \epsilon_0 \gamma_e + \epsilon_0 \Delta t^2 \omega_{ep}^2 \quad (46)$$

$$c_1 = \frac{2\mu_0 \Delta t^2 \omega_{mp}^2 - 8\mu_0}{C} \quad (47)$$

$$c_2 = \frac{4\mu_0 - 2\Delta t \mu_0 \gamma_m + \mu_0 \Delta t^2 \omega_{mp}^2}{C} \quad (48)$$

$$d_0 = \frac{4 + 2\Delta t \gamma_m}{C} \quad (49)$$

$$d_1 = \frac{-8}{C} \quad (50)$$

$$d_2 = \frac{4 - 2\Delta t \gamma_m}{C} \quad (51)$$

$$C = 4\mu_0 + 2\Delta t \mu_0 \gamma_m + \mu_0 \Delta t^2 \omega_{mp}^2. \quad (52)$$

Equations (26)–(31), (35)–(40) constitute the formulation of our proposed dispersive meshless method.

#### IV. NUMERICAL RESULTS

Here, two numerical examples are presented to investigate the efficiency of the proposed dispersive meshless method in comparison to a dispersive FDTD method.

##### A. 2-D Rectangular Resonator

We consider a 2-D rectangular cavity with dimensions  $1 \text{ m} \times 1 \text{ m}$ , perfectly conducting walls and Drude medium inside the cavity with the following parameters:  $\omega_p = 0$ ,  $\omega_{ep} = \omega_{mp} = \omega_p$ , and  $\gamma_e = \gamma_m = 0.0005\omega_0$ . We assume the modulated Gaussian pulse as the excitation current density; the Gaussian pulse is of the form

$$J = A \cos(2\pi f_0 t) \exp\left(-\left(\frac{t-t_0}{\tau}\right)^2\right) \hat{a}_x \quad (53)$$

where  $A = 1$ ,  $f = 0.4 \times 10^9 \text{ Hz}$ ,  $t_0 = 12 \times 10^{-9} \text{ s}$ , and  $\tau = 4 \times 10^{-9} \text{ s}$ . The angular frequency  $\omega_0$  is defined as  $\omega_0 = 2\pi f_0$ .

We represent the problem domain with a set of electric field nodes with regular distribution and consider a set of regularly distributed magnetic field nodes in such a way that each magnetic field node is surrounded by electric field nodes and vice versa. Moreover, we locate a set of electric-flux density nodes at the positions of electric field nodes and a set of magnetic-flux density nodes at the positions of magnetic field nodes. A point source is excited inside the cavity.

Fig. 1 shows the time variation of the electric field at an observation point inside the cavity obtained with the proposed dispersive meshless method.

1) *Resonant Frequency*: In order to obtain the resonant frequencies of the cavity, we applied the Fourier transform on the time response. On the other hand, to verify the accuracy of the proposed method, we ran the simulations for the mentioned cavity with a dispersive FDTD method.

In FDTD simulation, the spatial derivatives of Maxwell's equations are calculated by the finite difference approximation. Therefore, using a finer spatial resolution in comparison to the wavelength is necessary for accurate modeling of problems. The cell size should be smaller than  $\lambda/20$  to minimize the impact of any numerical dispersion on the results [19].

Here, for comparison, we have done two simulations through the dispersive FDTD method by considering two different grid sizes. In the former, the grid size is about  $\lambda/20$ , while the grid size is reduced and is about  $\lambda/30$  in the latter. Fig. 2 shows the resonant

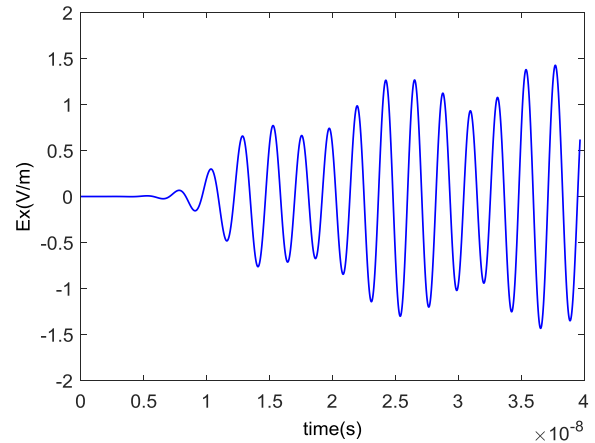


Fig. 1.  $E_x$  field recorded at an observation point inside the 2-D resonator solved with the proposed dispersive meshless method when  $t = 4 \times 10^{-8} \text{ s}$ .

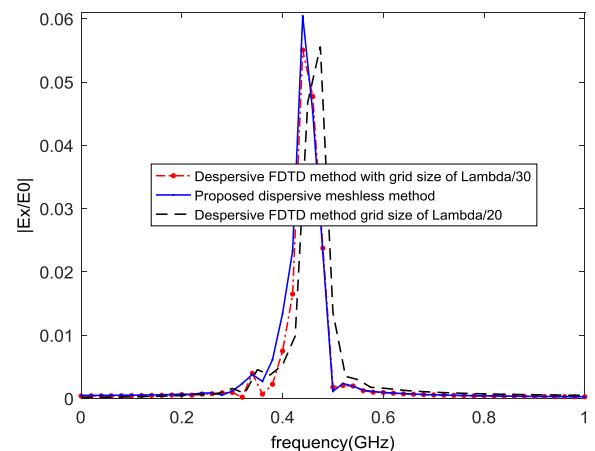


Fig. 2. Resonant frequencies obtained with the proposed dispersive meshless method and the dispersive FDTD method with two different cell sizes. Lambda shows the wavelength.

TABLE I  
COMPUTATIONAL COST FOR THE TWO METHODS

Method	Nodal spacing/grid size	Number of unknowns	Computational time(s)
Dispersive meshless	$\lambda/3$	25	0.7
Dispersive FDTD	$\sim \lambda/20$	784	1.75
	$\sim \lambda/30$	1600	3.1

frequencies obtained with the proposed dispersive meshless method and the dispersive FDTD method. In this Fig. 2, we use Lambda to denote the wavelength. The frequencies obtained using the dispersive FDTD method with the fine grid of  $\lambda/30$  shows a very good agreement with the results obtained through our proposed dispersive meshless method.

2) *Computational Cost*: Table I shows the computational cost of the proposed dispersive meshless method in comparison to the dispersive FDTD method.

In meshless method, the spatial derivatives of the electromagnetic fields are calculated using the analytical derivatives of their

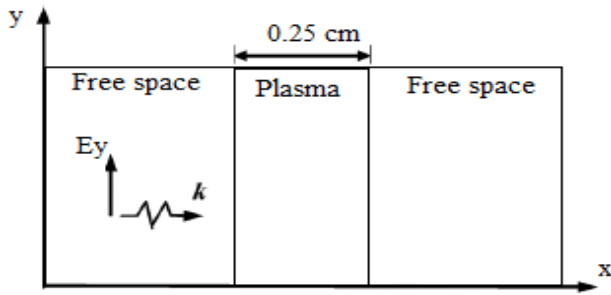


Fig. 3. Considered geometry of the plasma problem.

shape functions. Hence, the nodal spacing of meshless method can be far larger than that of the cell size of FDTD method without having any impact on the accuracy of the results. This property of meshless method can reduce the number of unknowns without changing the accuracy of the results.

According to the obtained results, considering a finer grid in the dispersive FDTD method leads to obtaining more accurate results which are in a good agreement with the results of simulation through our proposed dispersive meshless method. As Table I shows, the computational time of analysis of the problem through meshless method is considerably less than which is obtained using the dispersive FDTD method based on the fine grid of  $\lambda/30$ .

### B. Wave Propagation in a Dispersive Slab

In order to investigate the efficiency of our proposed method in modeling the frequency behavior of dispersive media, we have considered a 1-D problem which is consisted of a plasma slab, and the slab is located between free-space on both sides. We will calculate transient electromagnetic interactions with plasma using the proposed dispersive meshless method and ADE-FDTD method when a plane wave traveling in the plasma.

We have considered the excitation current density as follows:

$$J = \cos(2\pi f_0 t) \exp\left(-\left(\frac{t-t_0}{\tau}\right)^2\right) \hat{a}_y \quad (54)$$

where  $f_0 = 3 \times 10^9$  Hz,  $\tau = 1/(2f_0)$  and  $t_0 = 5\tau$ . The angular frequency  $\omega_0$  is defined as  $\omega_0 = 2\pi f_0$ .

The complex permittivity of the plasma medium is defined by the Drude dispersion model which is as follows:

$$\varepsilon(\omega) = 1 - \frac{\omega_{ep}^2}{\omega^2 - j\gamma_e\omega} \quad (55)$$

where  $\omega_{ep} = \omega_p$ ,  $\omega_p = 1.7815 \times 10^{10}$  rad/s, and  $\gamma_e = 2 \times 10^{10}$  rad/s. The geometry of the problem in Fig. 3 has been depicted, which shows that the thickness of the plasma slab is 0.25 cm. It is assumed that the length of the structure is not infinite just in the  $x$ -direction which is also direction of propagation.

In order to obtain the transmission coefficient of the incident wave, first, we have calculated the electric field versus time with both the ADE-FDTD method and the proposed dispersive meshless method. The transmitted field is the field which is obtained just in front of the plasma slab. The incident field versus time is the field which is obtained just behind the plasma slab when the slab is omitted. Then, we have obtained the frequency-domain responses of the transmitted and incident fields by applying the Fourier transform on their transient responses. Finally, the transmission coefficient is calculated by dividing the frequency-domain response of the transmitted field and the incident field.

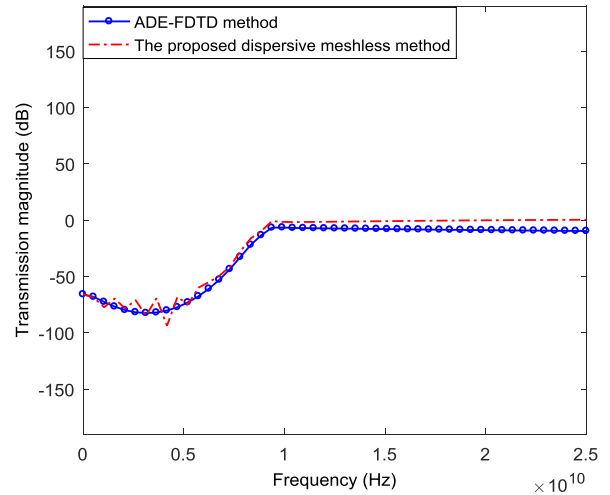


Fig. 4. Magnitude of transmission coefficient obtained from the Fourier transform of time-domain response when  $t = 1.92 \times 10^{-9}$  s.

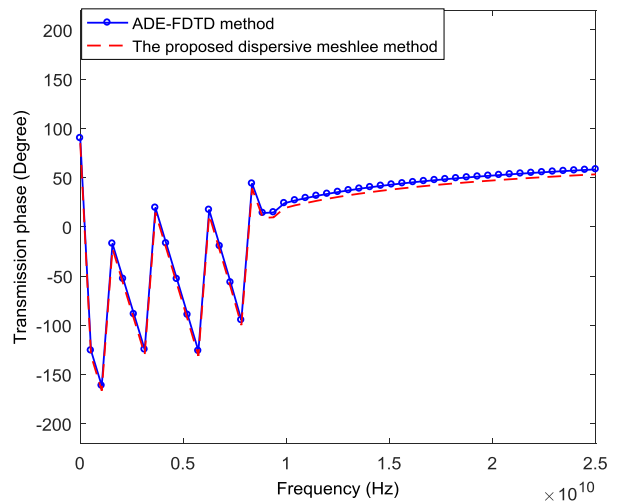


Fig. 5. Phase of transmission coefficient obtained from Fourier transform of time-domain response when  $t = 1.92 \times 10^{-9}$  s.

Figs. 4 and 5 show the magnitude and the phase of the transmission coefficient, respectively. According to Figs. 4 and 5, it can be observed that the obtained transmission coefficient with the proposed dispersive meshless method and ADE-FDTD method are in a good agreement.

## V. CONCLUSION

In this communication, we have proposed a 3-D dispersive meshless method for solving Maxwell's equations in a linear dispersive medium. We have used an ADE scheme to incorporate the frequency dispersion into the meshless method. Due to the capability of meshless methods in representing problems with complex geometries, the proposed dispersive meshless method can be more efficient than the conventional grid-based numerical techniques in simulating dispersive media with complex geometries. It is worth mentioning that although the formulation of our proposed meshless method is based on Drude dispersion model, the meshless method can be used for analysis of other dispersive materials by incorporating proper approaches into the meshless method; thus, this problem can be a topic for future studies.

## REFERENCES

- [1] R. J. Luebbers, F. Hunsberger, and K. S. Kunz, "A frequency-dependent finite-difference time-domain formulation for transient propagation in plasma," *IEEE Trans. Antennas Propag.*, vol. 39, no. 1, pp. 29–34, Jan. 1991.
- [2] R. Luebbers, D. Steich, and K. Kunz, "FDTD calculation of scattering from frequency-dependent materials," *IEEE Trans. Antennas Propag.*, vol. 41, no. 9, pp. 1249–1257, Sep. 1993.
- [3] A. Taflové and S. C. Hagness, *Computational Electrodynamics: The Finite-Difference Time-Domain Method*, 2nd ed. Boston, MA, USA: Artech House, 2000.
- [4] J.-M. Jin, *The Finite Element Method in Electromagnetics*, 2nd ed. New York, NY, USA: Wiley, 2002.
- [5] R. Luebbers, F. P. Hunsberger, K. S. Kunz, R. B. Standler, and M. Schneider, "A frequency-dependent finite-difference time-domain formulation for dispersive materials," *IEEE Trans. Electromagn. Compat.*, vol. 32, no. 3, pp. 222–227, Aug. 1990.
- [6] M. D. Bui, S. S. Stuchly, and G. I. Costache, "Propagation of transients in dispersive dielectric media," *IEEE Trans. Microw. Theory Techn.*, vol. 39, no. 7, pp. 1165–1172, Jul. 1991.
- [7] R. J. Hawkins and J. S. Kallman, "Linear electronic dispersion and finite-difference time-domain calculations: A simple approach (integrated optics)," *J. Lightw. Technol.*, vol. 11, no. 11, pp. 1872–1874, Nov. 1993.
- [8] F. Hunsberger, R. J. Luebbers, and K. S. Kunz, "Finite-difference time-domain analysis of gyrotropic media—I: Magnetized plasma," *IEEE Trans. Antennas Propag.*, vol. AP-40, no. 12, pp. 1489–1495, Dec. 1992.
- [9] R. Pontalti, L. Cristoforetti, R. Antolini, and L. Cescatti, "A multi-relaxation (FD)<sup>2</sup>-TD method for modeling dispersion in biological tissues," *IEEE Trans. Microw. Theory Techn.*, vol. MTT-42, no. 3, pp. 526–528, Mar. 1994.
- [10] C. Melon, P. Leveque, T. Monediere, A. Reineix, and F. Jecko, "Frequency dependent finite-difference-time-domain [(FD)<sup>2</sup>TD] formulation applied to ferrite material," *Microw. Opt. Technol. Lett.*, vol. 7, no. 12, pp. 577–579, 1994.
- [11] T. Kashiwa, Y. Ohtomo, and I. Fukai, "A finite-difference time-domain formulation for transient propagation in dispersive media associated with Cole-Cole's circular arc law," *Microw. Opt. Technol. Lett.*, vol. 3, no. 12, pp. 416–419, Dec. 1990.
- [12] T. Kashiwa and I. Fukai, "A treatment by the FD-TD method of the dispersive characteristics associated with electronic polarization," *Microw. Opt. Technol. Lett.*, vol. 3, no. 6, pp. 203–205, Jun. 1990.
- [13] R. M. Joseph, S. C. Hagness, and A. Taflové, "Direct time integration of Maxwell's equations in linear dispersive media with absorption for scattering and propagation of femtosecond electromagnetic pulses," *Opt. Lett.*, vol. 16, no. 18, pp. 1412–1414, Sep. 1991.
- [14] O. P. Gandhi, B.-Q. Gao, and J.-Y. Chen, "A frequency-dependent finite-difference time-domain formulation for general dispersive media," *IEEE Trans. Microw. Theory Techn.*, vol. 41, no. 4, pp. 658–665, Apr. 1993.
- [15] D. M. Sullivan, "Frequency-dependent FDTD methods using Z transforms," *IEEE Trans. Antennas Propag.*, vol. 40, no. 10, pp. 1223–1230, Oct. 1992.
- [16] G. R. Liu and Y. T. Gu, *An Introduction to Meshfree Methods and Their Programming*. New York, NY, USA: Springer, 2005.
- [17] S. J. Lai, B. Z. Wang, and Y. Duan, "Meshless radial basis function method for transient electromagnetic computations," *IEEE Trans. Magn.*, vol. 44, no. 10, pp. 2288–2295, Oct. 2008.
- [18] E. J. Kansa, "Multiquadrics—A scattered data approximation scheme with applications to computational fluid-dynamics—I surface approximations and partial derivative estimates," *Comput. Math. Appl.*, vol. 19, nos. 8–9, pp. 127–145, 1990.
- [19] Y. Hao and R. Mittra, *FDTD Modelling of Metamaterials: Theory and Applications*. Norwood, MA, USA: Artech House, 2008.
- [20] O. P. Gandhi, B.-Q. Gao, and J.-Y. Chen, "A frequency-dependent finite-difference time-domain formulation for induced current calculations in human beings," *Bioelectromagnetics*, vol. 13, no. 6, pp. 543–555, 1992.
- [21] Y. Yu and Z. Chen, "A 3-D radial point interpolation method for meshless time-domain modeling," *IEEE Trans. Microw. Theory Techn.*, vol. 57, no. 8, pp. 2015–2020, Aug. 2009.